

A Three-Dimensional CFD Analyses for the Gas Holdup in a Bubble Column Reactor

M. W. Abdulrahman¹, N. Nassar²

¹Rochester Institute of Technology (RIT)
Dubai, UAE

mwacad@rit.edu; nin8507@g.rit.edu

²Rochester Institute of Technology (RIT)
Dubai, UAE

Abstract - Hydrogen is becoming an increasingly attractive alternative fuel. As such it is important to investigate different methods of hydrogen production. This paper examines the thermochemical process of splitting water using the three stage Cu-Cl Cycle. In particular it examines the hydrodynamics of the direct contact heat transfer in the Cu-Cl's oxygen reactor for a two-phase system, using a three dimensional Eulerian-Eulerian Computational Fluid Dynamics (CFD) model. The model is verified using experimental results and compared to a two-dimensional CFD model by examining the gas holdup using a helium-water system for different superficial gas velocities (0.05-0.15 m/s). The three-dimensional helium-water system is able to accurately model the trends of the gas holdup while changing the superficial gas velocity with a maximum percent error of 8.37%. The three-dimensional model is more accurate and somewhat over predicted in comparison to the two-dimensional model. Also, it is found that gas holdup increases when increasing the superficial gas velocity.

Keywords: gas holdup; hydrodynamics; Cu-Cl cycle; CFD; hydrogen

1. Introduction

The world heavily relies on fossil fuels to generate energy. Unfortunately, energy produced from fossil fuels leads to the release of harmful greenhouse gases which can degrade and pollute the environment. One solution which has the potential to generate energy as an alternative to fossil fuels is hydrogen. Thermochemical cycles are potential solutions that can be coupled with nuclear reactors to thermally breakdown water into oxygen and hydrogen through multistage processes. Argonne National Laboratories (ANL) has recognized the copper-chlorine (Cu-Cl) cycle as one of the most promising low temperature cycles [1-2]. The CuCl cycle's oxygen generation step is an endothermic process that requires a reaction heat of 129.2 kJ/mol and a temperature of 530°C [3]. As a result, heat must be provided to increase and maintain the temperature of the reactor's mass. Different methods of heat transfer have been investigated for the oxygen reactor. It has been found that the best method of heat transfer that can be used for the oxygen reactor is the direct contact heat transfer from the oxygen gas to the molten CuCl [4-9] using a Bubble Column Reactor (BCR). Bubble columns are advantageous as they can be used in a variety of industrial applications. Scaling up, modeling, and designing of bubble columns is a complex process as because it requires detailed knowledge in relation to kinetics, hydrodynamics, heat and mass transfer, chemical reaction rates, phase holdup, flow regimes, pressure change, and solid distribution. One of the most important characteristics to describe a bubble columns' performance is the gas holdup [10]. Gas holdup is a dimensionless parameter that represents the volume fraction of the gas in the BCR. The objective of this paper is to investigate numerically, using 3D CFD simulations, the multiphase hydrodynamics of a direct contact heat transfer reactor between the O₂ gas bubbles and the molten CuCl salt in the oxygen reactor of the Cu-Cl cycle.

Over the years research has been conducted in relation to bubble column reactors both experimentally and numerically. Abdulrahman et. al. [11] have reviewed the Eulerian approach to CFD analyses for bubble column reactors. Abdulrahman [12-16] has investigated the 2D CFD simulations for the gas holdup, volumetric heat transfer coefficient, gas and slurry temperatures, and the solid concentration of the bubble column reactor. Matiazzo [17] conducted a 3D CFD investigation of a gas-liquid flow in a churn turbulent regime in order to compare the effectiveness of several models in relation to predicting the drag closures, breakup, and coalescence. Ertekin et al. [18] validated the hydrodynamic CFD models presented by Fletcher et al. (2016) while varying conditions such as column diameter from 0.19 m to 3m and the superficial gas velocities which varied from 0.03 m/s to 0.25 m/s based on the experimental data of Raimundo et al. (2019) and Mclure et al. (2014). Yan et al. [19] used three different optimized drag models to simulate the hydrodynamics of a high pressure, air-water bubble column. The effects of changing the superficial gas velocities (0.121, 0.174, 0.233 and 0.296 m/s) and the effects of changing the reactors pressure (0.5, 1.0, 1.5 and 2.0 MPa) on the

radial gas holdup were investigated. The data was investigated using 2D and 3D CFD simulations and compared to experimental calculated data using the electrical resistance tomography method. Adam and Tuwaechi [20] generated a 2 phase, gas - liquid, Eulerian- Eulerian, k- ϵ mixture turbulence CFD model, to study the effects of gas holdup and superficial gas velocity on the hydrodynamics using a course and fine mesh. From the CFD model it was observed that as the time step increased so did the volume fraction. The finer mesh with a grid resolution of 0.005 led to a clearer observation. Pourtousi et al. [21] investigated the bubble column regime and the effects of changing superficial gas velocity (0.0025 – 0.015 m/s) and varying bubble diameters (3, 4, 5 and 5.5mm) on the Euler-Euler simulation flow pattern predictions. A 3D air water CFD simulation was created with a slurry bubble column with a height of 2.6m and diameter of 0.288m.

As a result of the above examination of the literatures, it can be concluded that 3D CFD simulations of the thermal hydraulics for the oxygen slurry bubble column reactor with direct contact heat transfer in the Cu-Cl cycle have not been investigated before. Additionally, it is found that prior CFD studies on slurry bubble column reactors explored the hydrodynamics of the reactors using PBM models and the heat transmission of the reactors through indirect heat transfer from inside objects. This paper will address the aforementioned gaps by performing 3D CFD simulations of the slurry bubble column reactor's hydrodynamics with direct contact heat transfer at the operating conditions of the oxygen reactor in the Cu-Cl cycle.

2. CFD Simulation Model

2.1. Bubble Column Reactor Geometry

The simulations of this paper are validated against the experimental data provided by Abdulrahman [9, 22-25]. As such the simulated reactor is designed to be a simplified version of the physical reactor to reduce computational costs. The experimental reactor was constructed of stainless steel with a diameter of 21.6 cm and a column height of 91.5 cm. A stainless-steel distributor is inserted 10.8 cm above the base of the SBCR. The gas was fed into the SBCR using a six-arm sparger type gas distributor. Each arm of the sparger had 12 orifices with 0.3 cm diameters (72 holes in total). In order to reduce computational costs, the shape of the reactor is simplified in the CFD simulations (Fig. 1).

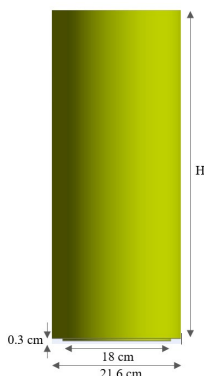


Fig. 1 Schematic diagram of the reactor design

2.2 Material Properties

The experiments carried out by Abdulrahman [9, 22-25] were conducted on a Water-Helium-Alumina system due to challenges associated with the Cuprous Chloride (CuCl) and Oxygen (O₂) materials. The challenges include: the difficulties in viewing O₂ bubbles in melted CuCl due to its dark colors, the corrosiveness of the CuCl molten salt, and the O₂ gas ability to oxidize many materials to accelerate its combustion [9, 26-27]. Based on Buckingham pi theorem, a dimensional analysis was conducted which identified liquid water at 22°C and Helium gas at 90°C to be suitable alternatives to molten CuCl at 530°C and oxygen gas at 600°C [9]. The physical properties for He gas and liquid water are shown in Table 1 [28-29].

Table 1: Material properties for the Helium gas and liquid Water.

| Physical Property | Units | Gas Phase (He) | Liquid Phase (H ₂ O) |
|------------------------------|-------|------------------|---------------------------------|
| Temperature (T) | | | |
| Temperature (T) | | | |
| Density (ρ) | | | |
| Specific Heat (C_p) | | | |
| Thermal Conductivity (k) | | | |
| Dynamic Viscosity (μ) | | 10 ⁻⁵ | 0.00075 |
| Molecular Weight | mol | 4 | 18 |
| Standard State Enthalpy | mol | 0 | 0 |
| Surface Tension (σ) | | | |

2.3. CFD Simulations Theory

The CFD simulations in this paper are performed for a 3D plane system with Eulerian-Eulerian model, Eulerian sub-model, and pressure-based solver type. The equations used in the CFD analysis of this paper are shown in Table 2. The equations in Table 2 are written for gas phase only. For liquid phase, the equations are similar to the gas phase, therefore, they are not repeated.

Table 2: Details of equations used in the 3D CFD simulations.

| Description [reference] | Equation |
|--------------------------------------------------------------------|-------------------------------------------------------------------------------------------------------------------------------------------------------------------------------------------------------------------------------------------------------------------------------------------------------------------------------------------------------------------------------------------------------------------------------------------------------------------------------------------------------------------------------------------------------------------------------------------------------------------------------------------------------------------------------------------------------------------------------------------------------------------------------------------------------------------------------------------------------------------------------------------------------------------------------------------------------------------------------------------------------------------------------------------------------------------------------------------------------------------------------------------------------------------------------------------------------------------------------------------------------------------------------------------------------------------------------------------------------------------------------------------------------------------------------------------------------------------------------------------------------------------------------------------------------------------------------------------------------------------------------------------------------------------------------------------------------------------------------------------------------------------------------------------------------------------------------------------------|
| Volume equation [30] | $\int_V \alpha_g dV$ |
| Continuity equation in 3D Polar coordinates (r, θ, y) [9] | $\frac{\partial v_{r,g}}{\partial r} + \frac{v_{r,g}}{r} + \frac{1}{r} \frac{\partial v_{\theta,g}}{\partial \theta} + \frac{\partial v_{y,g}}{\partial y} = 0$ |
| Momentum equation in 3D Polar coordinates [9] | $\frac{\partial v_r}{\partial t} + v_r \frac{\partial v_r}{\partial r} + \frac{v_\theta}{r} \frac{\partial v_r}{\partial \theta} + v_y \frac{\partial v_r}{\partial y} - \frac{v_\theta^2}{r} = -\alpha_g \frac{\partial P}{\partial r} + \alpha_g \frac{\mu_{g,eff}}{3} \frac{\partial(\nabla \cdot \mathbf{V})}{\partial r} +$ $\alpha_g \left[\frac{1}{r} \frac{\partial}{\partial r} \left(r \frac{\partial v_r}{\partial r} \right) + \frac{1}{r^2} \frac{\partial^2 v_r}{\partial \theta^2} + \frac{\partial^2 v_r}{\partial y^2} - \frac{v_r}{r^2} - \frac{2}{r^2} \frac{\partial v_\theta}{\partial \theta} \right] + \rho_g \alpha_g g_r + M_{i,g,r}$ $\frac{\partial v_\theta}{\partial t} + v_r \frac{\partial v_\theta}{\partial r} + \frac{v_\theta}{r} \frac{\partial v_\theta}{\partial \theta} + v_y \frac{\partial v_\theta}{\partial y} + \frac{v_r v_\theta}{r} = -\alpha_g \frac{1}{r} \frac{\partial P}{\partial \theta} + \alpha_g \frac{\mu_{g,eff}}{3r} \frac{\partial(\nabla \cdot \mathbf{V})}{\partial \theta} +$ $ff \left[\frac{1}{r} \frac{\partial}{\partial r} \left(r \frac{\partial v_\theta}{\partial r} \right) + \frac{1}{r^2} \frac{\partial^2 v_\theta}{\partial \theta^2} + \frac{\partial^2 v_\theta}{\partial y^2} + \frac{2}{r^2} \frac{\partial v_r}{\partial \theta} - \frac{v_\theta}{r^2} \right] + \rho_g \alpha_g g_\theta + M_{i,g,\theta}$ $\frac{\partial v_y}{\partial t} + v_r \frac{\partial v_y}{\partial r} + \frac{v_\theta}{r} \frac{\partial v_y}{\partial \theta} + v_y \frac{\partial v_y}{\partial y} = -\alpha_g \frac{\partial P}{\partial y} + \alpha_g \mu_{g,eff} \left[\frac{1}{r} \frac{\partial}{\partial r} \left(r \frac{\partial v_y}{\partial r} \right) + \frac{1}{r^2} \frac{\partial^2 v_y}{\partial \theta^2} \right] -$ $\rho_g \alpha_g g_y + M_{i,g,y}$ |
| Energy equation in 3D Polar coordinates | $\left(\frac{\partial T_g}{\partial t} + v_{r,g} \frac{\partial T_g}{\partial r} + \frac{v_{\theta,g}}{r} \frac{\partial T_g}{\partial \theta} + v_{y,g} \frac{\partial T_g}{\partial y} \right) = \bar{\tau}_g : \nabla V_g + k_g \left(\frac{1}{r} \frac{\partial}{\partial r} \left(r \frac{\partial T_g}{\partial r} \right) + \frac{1}{r^2} \frac{\partial^2 T_g}{\partial \theta^2} \right) -$ $S_g + Q_{g,sl}$ |

| | | |
|----------------------------------|-------------------------------------------------|------------------|
| Gas density | ρ_g | |
| Force [30] | $\frac{\rho_g f}{6 \tau_b} d_b A_i (V_g - V_l)$ | |
| Specific area [30] | $\frac{\alpha_g (1 - \alpha_g)}{d_b}$ | |
| Carman-Kozeny drag equation [30] | $\frac{24 (1 + 0.15 Re_b^{0.687})}{Re_b}$ | $Re_b \leq 1000$ |
| | 0.44 | $Re_b > 1000$ |

2.4. Turbulence Model

The Reynolds-Averaged Navier-Stokes (RANS) models, such as k- ϵ and k- ω , are the least computationally expensive approaches for estimating complex turbulent flows. They are capable of simulating a broad variety of turbulent flows and heat transfer processes with an acceptable accuracy. The RNG k- ϵ is similar to the standard k- ϵ model however, for a larger range of flows the RNG k- ϵ it is more accurate and reliable [30]. The RNG k- ϵ model is selected for this study as the flow regime will be a churn turbulent flow, which is best simulated with the RNG k- ϵ model. The K- ϵ sub model that is used in this study is the dispersed turbulence model due to the significant difference in the phase densities between liquid and gas and because the gas phase concentrations are low. Also, turbulence model is less computationally expensive than the per-phase turbulence model. The wall function that is used in this paper is the standard wall function because it is prominently used for industries and provides reasonable results for a variety of wall bounded flows [30].

2.5. ANSYS Fluent Setup and Boundary Conditions

The software used to simulate the 3D SBCR is ANSYS 2021 R1. A hexahedron mesh is used for the BCR. The mesh independence is conducted to ensure that the largest mesh size is selected to minimize the computational expenses while achieving acceptable results. The final mesh is composed of 26,825 nodes and 24,396 elements. This led to a 3% difference in the gas holdup when using finer meshes.

There are three boundaries in the simulated SBCR, the inlet, outlet and the wall conditions. The single inlet boundary condition is set with a specified superficial gas velocity and assumed to have a gas holdup of 1. The outlet pressure is set to atmospheric pressure. A no slip condition is applied to the walls of the reactor for both phases. The turbulent kinetic energy and dissipation rate at the inlet and outlet were specified using 5,000 iterations as they are difficult to estimate for turbulent models.

3. Results

The 3D CFD simulations are conducted for the Helium-Water System. The system is investigated to ascertain the effect of varying the superficial gas velocity (U_{gs}) on the gas holdup (α_g) of the system. Additionally, the Helium-Water system results are compared to previous experimental data and 2D CFD simulated data. Fig. 2 depicts the effects of varying the superficial gas velocity (U_{gs}) on the average gas holdup (α_g) for a helium-water system. From the figure, it can be observed that increasing U_{gs} leads to a higher α_g for different reactor heights. Figures 3 & 4 show the contours of the cut sections of the BCR taken in the center of the XY, and ZY planes. Additional cut sections are taken at various heights on the ZX plane within the reactor at heights 10, 20 and 30 cm from the base of the reactor to allow for a more detailed contour of α_g . It is clear from the contours that the gas holdup is not symmetrical on the XY, ZY and the ZX planes demonstrating that the behavior of the gas holdup is strongly three dimensional. It is observed that α_g increases when U_{gs} increases. This is because a larger number of bubbles are formed with the increased gas velocity. Larger bubbles can then be formed due to coalescence which results in an increase in gas holdup. Additionally, a pressure drop in the bed of the reactor occurs due to a decrease in the hydrostatic pressure. The higher the gas flow rate the lower the hydrostatic pressure which further decrease the bed pressure and increases α_g [9].

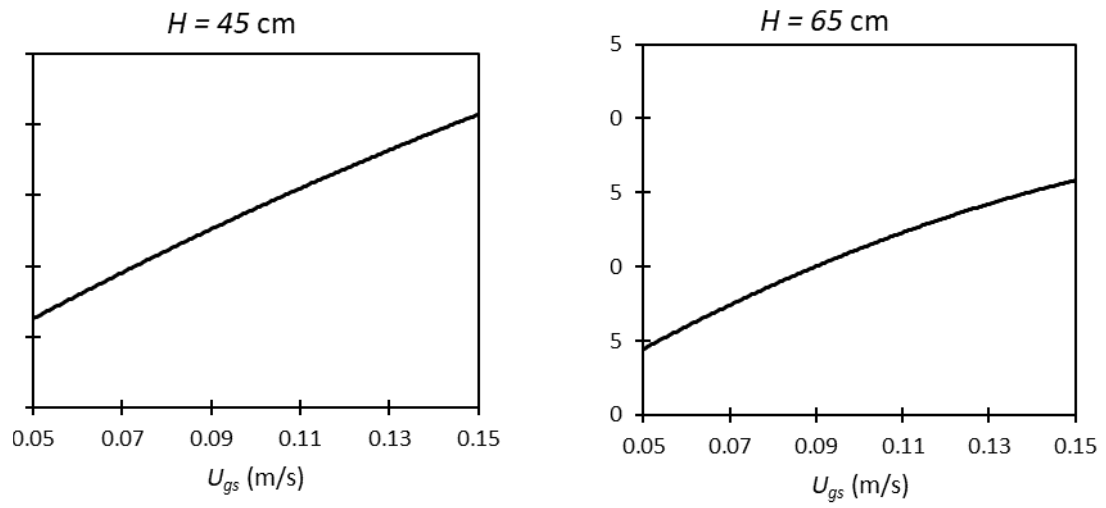


Fig. 2 Average Gas Holdup Versus Superficial Gas Velocity of Helium-Water System for Different Static Liquid Heights.

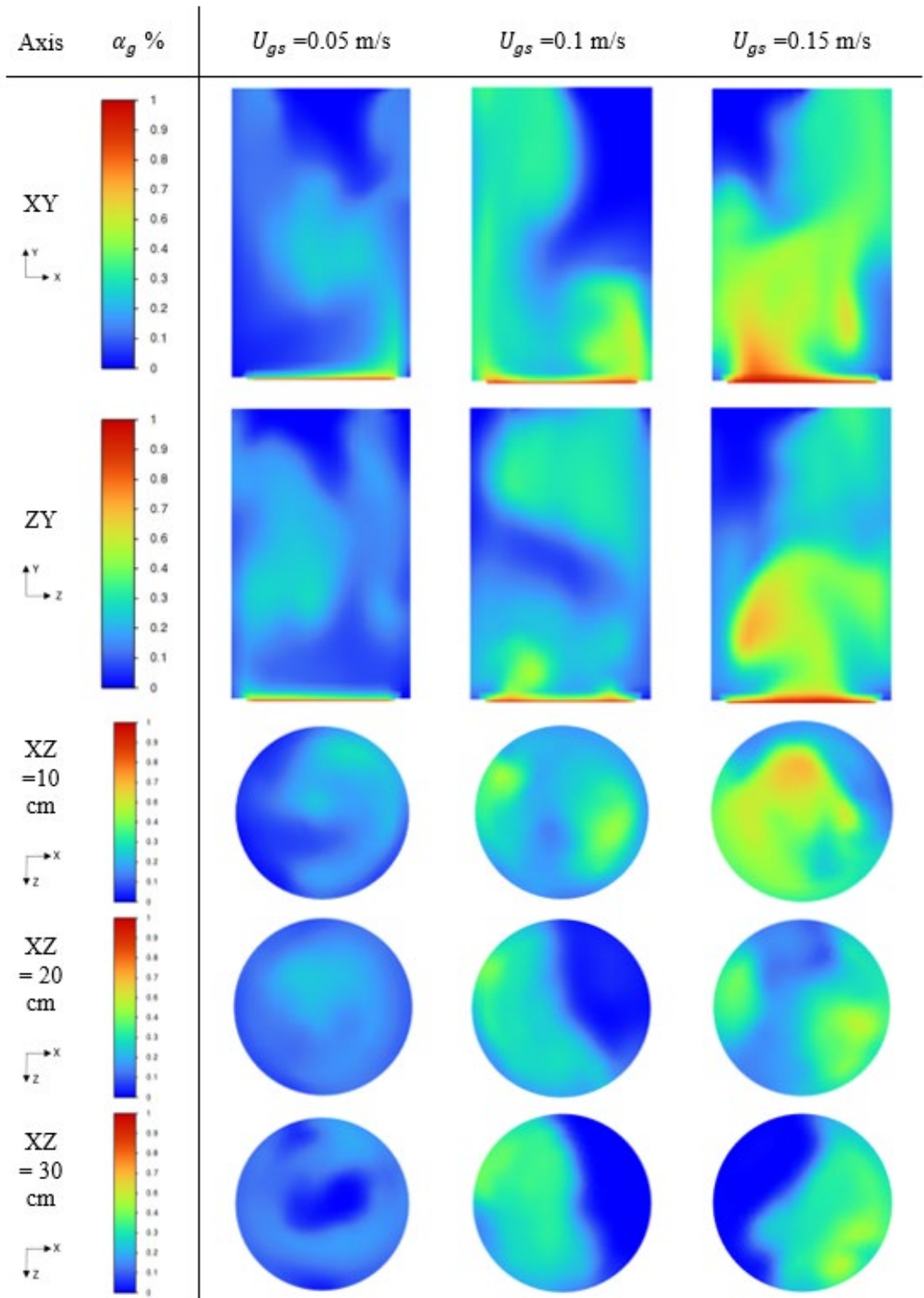


Fig. 3 Water- Helium-Alumina Gas Holdup Contours for H=45cm.

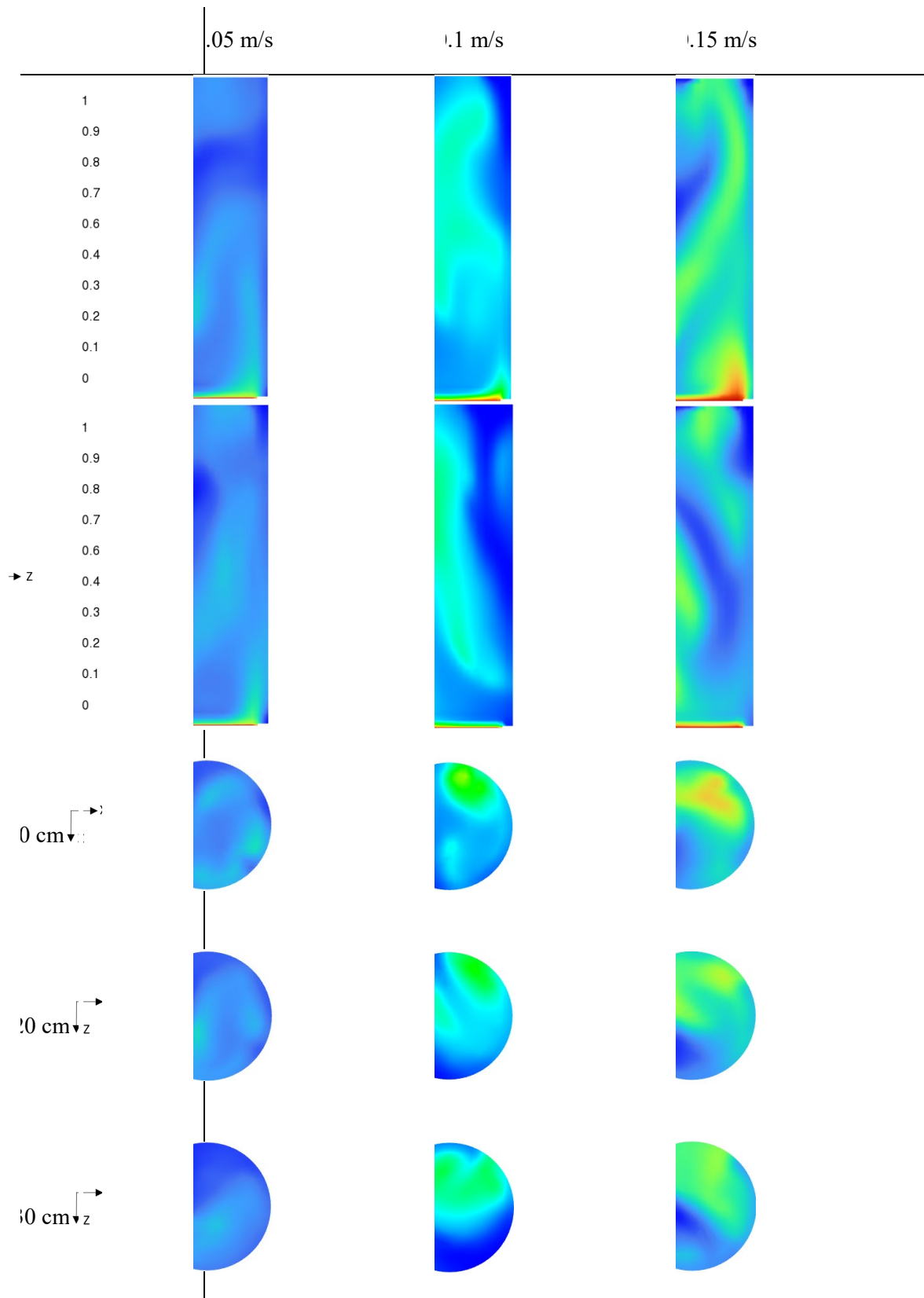


Fig. 4 Water- Helium-Alumina Gas Holdup Contours for H=65cm.

The gas holdup data of the 3D-CFD Helium-Water BC simulations were validated against experimental data conducted by Abdulrahman [9] and compared to 2D simulations conducted by Abdulrahman [9]. The effects of static liquid height, and superficial gas velocity on the gas holdup are compared in Fig. 5. It can be noted that the majority of

the gas holdup results from the simulations were overpredicted. The 3D simulations for the Helium-Water had a maximum relative error less than 8.4%. This is a significant improvement over the 2D-CFD simulations which had at most a maximum relative error of less than 28.5% and the majority of the results were underpredicted [9]. Potential methods to reduce the relative error is to decrease the mesh size. Decreasing the mesh size will allow the software to take into consideration small vortical structures in the flow such as eddies [32]. The mesh size that is used in this study is to reduce the computational cost.

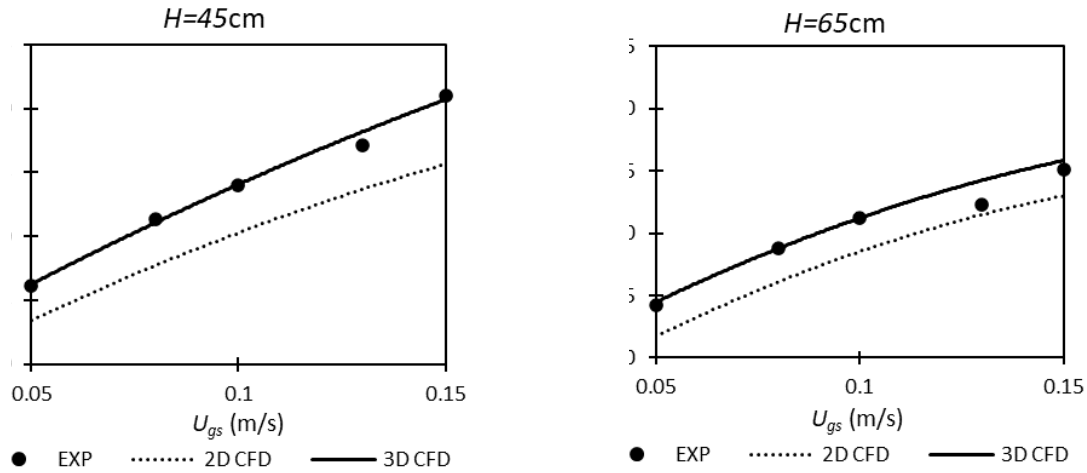


Fig. 5 Comparison of the average Gas Holdup versus superficial gas velocity of the Helium-Water-Alumina 3D CFD simulations with 2D CFD simulations and experimental data.

5. Conclusions

The objective of this paper is to study the gas holdup of the Oxygen Bubble Column Reactor in the thermochemical Cu-Cl cycle of hydrogen production. ANSYS Fluent software is utilized to conduct 3D-CFD simulations to validate the model for a Water- Helium system at different superficial gas velocities. Several key takeaways can be concluded from the CFD simulations of this paper. The conclusions include:

- Gas holdup flow patterns in a 3D, CFD simulation, within a BCR are non-symmetrical.
- Gas holdup increases with increasing superficial gas velocities for different reactor heights.

For the 3D-CFD results of Helium-Water system, gas holdup is somewhat overpredicted the experimental results, opposed to 2D simulations which were underpredicted the experimental results.

The 3D simulations of the Helium-Water system are more accurate than that of 2D-CFD simulations.

List of Symbols

| | | | |
|-----------|-----------------------------------------|-------------------------|----------------------------------------------|
| A_i | cial area concentration | | ty field |
| C | ic heat | | es of gas |
| | oefficient | | es of liquid |
| | > diameter | U_{gs} | icial gas velocity |
| | ational acceleration | | ldup |
| | nterfacial forces between the phases | μ_{eff} | ve viscosity |
| | pressure | μ_g | ic viscosity gas |
| $Q_{g,l}$ | ty of heat exchange between the gas and | μ_l | ic viscosity liquid |
| | lds number | ρ_g | y, gas |
| | perature | ρ_l | y, liquid |
| | | $\bar{\tau} : \nabla V$ | is stress tensor contracted with the v it |

References

- [1] Lewis, M. A., M. Serban, and J. K. Basco. "Generating hydrogen using a low temperature thermochemical cycle." *Proceedings of the ANS/ENS 2003 Global International Conference on Nuclear Technology, New Orleans*. 2003.
- [2] Serban, M., M. A. Lewis, and J. K. Basco. "Kinetic study of the hydrogen and oxygen production reactions in the copper-chloride thermochemical cycle." *AIChE 2004 spring national meeting, New Orleans, LA*. 2004.
- [3] Ryskamp, J.M., Hildebrandt, P., Baba, O., Ballinger, R., Brodsky, R., Chi, H.W., Crutchfield, D., Estrada, H., Garnier, J.C., Gordon, G. and Hobbins, R. *Design Features and Technology Uncertainties for the Next Generation Nuclear Plant*. No. INEEL/EXT-04-01816. Idaho National Laboratory (INL), 2004.
- [4] Abdulrahman, Mohammed W. "Similitude for Thermal Scale-up of a Multiphase Thermolysis Reactor in the Cu-Cl Cycle of a Hydrogen Production." *International Journal of Energy and Power Engineering*, vol. 10.5, 2016, pp. 664-670.
- [5] Abdulrahman, Mohammed W. "Heat Transfer Analysis of a Multiphase Oxygen Reactor Heated by a Helical Tube in the Cu-Cl Cycle of a Hydrogen Production." *International Journal of Mechanical and Mechatronics Engineering*, vol. 10.6, 2016, pp. 1122-1127.
- [6] Abdulrahman, M. W., Wang, Z., Naterer, G. F., & Agelin-Chaab, M. "Thermohydraulics of a thermolysis reactor and heat exchangers in the Cu-Cl cycle of nuclear hydrogen production." in *Proceedings of the 5th World Hydrogen Technologies Convention*, 2013.
- [7] Abdulrahman, Mohammed W. "Heat Transfer Analysis of the Spiral Baffled Jacketed Multiphase Oxygen Reactor in the Hydrogen Production Cu-Cl Cycle." In *Proceedings of the 9th International Conference on Fluid Flow, Heat and Mass Transfer (FFHMT'22)*, 2022.
- [8] Abdulrahman, Mohammed W. "Review of the Thermal Hydraulics of Multi-Phase Oxygen Production Reactor in the Cu-Cl Cycle of Hydrogen Production." In *Proceedings of the 9th International Conference on Fluid Flow, Heat and Mass Transfer (FFHMT'22)*, 2022.
- [9] Abdulrahman, Mohammed W. *Analysis of the thermal hydraulics of a multiphase oxygen production reactor in the Cu-Cl cycle*. Diss. University of Ontario Institute of Technology (Canada), 2016.
- [10] Shaikh, Ashfaq. *Bubble and slurry bubble column reactors: mixing, flow regime transition and scaleup*. Vol. 68. No. 09. 2007.
- [11] Abdulrahman, Mohammed W., and Nibras Nassar. "Eulerian Approach to CFD Analysis of a Bubble Column Reactor-A." In *Proceedings of the 8th World Congress on Mechanical, Chemical, and Material Engineering (MCM'22)*, 2022.
- [12] Abdulrahman, Mohammed W. "CFD Simulations of Gas Holdup in a Bubble Column at High Gas Temperature of a Helium-Water System." In *Proceedings of the 7th World Congress on Mechanical, Chemical, and Material Engineering (MCM'20)*, 2020
- [13] Abdulrahman, M.W. "CFD Simulations of Direct Contact Volumetric Heat Transfer Coefficient in a Slurry Bubble Column at a High Gas Temperature of a Helium-Water-Alumina System." *Applied Thermal Engineering*, vol. 99, 2016, pp. 224-234.
- [14] Abdulrahman, Mohammed W. "CFD Analysis of Temperature Distributions in a Slurry Bubble Column with Direct Contact Heat Transfer." In *Proceedings of the 3rd International Conference on Fluid Flow, Heat and Mass Transfer (FFHMT'16)*. 2016.
- [15] Abdulrahman, Mohammed W. "Temperature profiles of a direct contact heat transfer in a slurry bubble column." *Chemical Engineering Research and Design*, vol. 182, 2022, pp. 183-193.
- [16] Abdulrahman, Mohammed W. "Effect of Solid Particles on Gas Holdup in a Slurry Bubble Column." In *Proceedings of the 6th World Congress on Mechanical, Chemical, and Material Engineering*, 2020.
- [17] Matiazzo, T., Decker, R.K., Bastos, J.C.S.C., Silva, M.K. and Meier, H. "Investigation of Breakup and Coalescence Models for Churn-Turbulent Gas-Liquid Bubble Columns." *Journal of Applied Fluid Mechanics* 13.2 (2020): 737-751.
- [18] Ertekin, E., Kavanagh, J.M., Fletcher, D.F. and McClure, D.D. "Validation studies to assist in the development of scale and system independent CFD models for industrial bubble columns." *Chemical Engineering Research and Design* 171 (2021): 1-12.
- [19] Yan, P., Jin, H., He, G., Guo, X., Ma, L., Yang, S. and Zhang, R. "CFD simulation of hydrodynamics in a high-pressure bubble column using three optimized drag models of bubble swarm." *Chemical Engineering Science* 199

- (2019): 137-155.
- [20] Adam, Salman, and Kalthoum Tuwaechi. "Hydraulic Simulation of Bubble Flow in Bubble Column Reactor." *Journal of Complex Flow* 1.2 (2019).
- [21] Pourtousi, M., P. Ganesan, and J. N. Sahu. "Effect of bubble diameter size on prediction of flow pattern in Euler–Euler simulation of homogeneous bubble column regime." *Measurement* 76 (2015): 255-270.
- [22] Abdulrahman, M. W. "Experimental studies of gas holdup in a slurry bubble column at high gas temperature of a helium–water–alumina system." *Chemical Engineering Research and Design* vol. 109, 2016, pp. 486-494.
- [23] Abdulrahman, M. W. "Experimental studies of the transition velocity in a slurry bubble column at high gas temperature of a helium–water–alumina system." *Experimental Thermal and Fluid Science*, vol. 74, 2016, pp. 404-410.
- [24] Abdulrahman, M. W. "Experimental studies of direct contact heat transfer in a slurry bubble column at high gas temperature of a helium–water–alumina system." *Applied Thermal Engineering*, vol. 91, 2015, pp. 515-524.
- [25] Abdulrahman, Mohammed Wassef. "Direct contact heat transfer in the thermolysis reactor of hydrogen production Cu—Cl cycle." U.S. Patent No. 10,059,586. 28 Aug. 2018.
- [26] Abdulrahman, Mohammed Wassef. "Material substitution of cuprous chloride molten salt and oxygen gas in the thermolysis reactor of hydrogen production Cu—Cl cycle." U.S. Patent No. 10,526,201. 7 Jan. 2020.
- [27] Abdulrahman, Mohammed W. "Simulation of Materials Used in the Multiphase Oxygen Reactor of Hydrogen Production Cu-Cl Cycle." *Proceedings of the 6th International Conference of Fluid Flow, Heat and Mass Transfer (FFHMT'19)*. 2019.
- [28] Borgnakke, Claus, and Richard E. Sonntag. "Fundamentals of thermodynamics: Part 1." (2009).
- [29] Petersen, Helge. *The properties of helium: density, specific heats, viscosity, and thermal conductivity at pressures from 1 to 100 bar and from room temperature to about 1800 K*. Copenhagen: Jul. Gjellerup, 1970.
- [30] *ANSYS FLUENT Theory Guide*, Release 14.5. (2012). ANSYS, Inc.
- [31] L. Schiller, A. Naumann, *Über die grundlegenden berechnungen bei der schwerkraftaufbereitung / About the basic calculations in the gravity-treatment*, *Zeitung des vereins deutscher ingenieure / Newspaper of the Association of German Engineers*, 1933, pp. 77–318.
- [32] Sokolichin, A., and Gs Eigenberger. "Applicability of the standard $k-\epsilon$ turbulence model to the dynamic simulation of bubble columns: Part I. Detailed numerical simulations." *Chemical Engineering Science* 54.13-14 (1999): 2273-2284.